SF2A 2024
M. Béthermin, K. Baillié, N. Lagarde, J. Malzac, R.-M. Ouazzani, J. Richard, O. Venot, A. Siebert (eds)

SATURN'S FORMATION AT THE CARBON DIOXIDE ICELINE

A. Aguichine[1] and O. Mousis[2]

Abstract. Giant planets of the solar system exhibit supersolar metallicities of volatile elements. It is believed that the heavy element content was acquired from the protoplanetary disk when the planets were formed. However, the source and nature of volatile compounds accreted by giant planets are still under debate. In this work, we use the metallicity and composition of the protosolar nebula (PSN) to infer the origin of the building blocks of Saturn based on currently available measurements of its atmospheric composition and bulk metallicity inferred from models. The metallicity profile is computed from a 1+1D state-of-the-art model that includes radial transport of volatile compounds and phase changes between pure ices and their corresponding vapors. Our model demonstrates that the bulk metallicity of Saturn is more accurately reproduced in the vicinity of the CO_2 iceline. Furthermore, our model calculates the composition of the PSN across varying heliocentric distances and time intervals. Leveraging this data, we offer a spectrum of elemental abundances anticipated within Saturn's atmosphere, including enrichments of noble gases that can be quantified via an in situ probe.

Keywords: Planet formation, Saturn, protosolar nebula, planet composition

1 Introduction

Giant planets of the solar system exhibit an increasing metallicity with heliocentric distance (Guillot 2005; Helled et al. 2011; Nettelmann et al. 2013). This trend is verified for both the bulk metallicity inferred by interior structure models, defined as the total heavy-element content in the planet (core and envelope), and volatile abundances in their atmospheres obtained by remote and in situ measurements. Saturn has an intermediate position both in terms of semi-major axis and metallicity (Vazan et al. 2016; Militzer et al. 2019; Movshovitz et al. 2020; Ni 2020; Mankovich & Fuller 2021). For most planetary formation models, reproducing Saturn's volatile content represents a highly fine-tuned problem, since models usually rely on a multitude of independent parameters that control various mechanisms that directly impact the composition of the planet (Hubickyj et al. 2005; Levison et al. 2010; Schneider & Bitsch 2021). Since both Saturn and Jupiter are members of the gas giants family, it is possible that both planets formed in a similar way, and that the differences in their metallicities are the result of the specificity of the regions where each planet formed.

In this work, we extend the concept of planetary formation at specific icelines to the case of Saturn, with the possibility that Saturn may have formed in the vicinity of either the CO or CO_2 iceline, and our goal is to investigate the implications for the final composition of Saturn. To do so, we perform a quantitative analysis using the 1D disk evolution model from Aguichine et al. (2020, 2022), that includes the evolution of both the H_2-He cloud, and the dynamics of up to 13 species, where 12 volatile species are chosen as the main carriers of C, N, O, P, S, Ar, Kr, and Xe, and the last phase accounts for silicate grains. We use the results of our model to derive possible formation time and location of Saturn based on its total heavy-element content, which we use to provide constraints on volatile abundances, in particular for noble gases.

2 Methods

2.1 Composition of Saturn

We consider the elemental abundances of C, N, and P abundances from Fletcher et al. (2009b), Fletcher et al. (2011), and Fletcher et al. (2009a), respectively. These abundances are reported as follows: C/H=

[1] Department of Astronomy and Astrophysics, University of California, Santa Cruz, CA, USA
[2] Aix-Marseille Université, CNRS, CNES, Institut Origines, LAM, Marseille, France

9.61±0.59, N/H= 2.05±1.44, and P/H= 11.2±1.3 times their respective protosolar values. The N abundance is determined from models assuming the presence of NH_4HS clouds, resulting in a lower atmospheric N abundance compared to the expected bulk N abundance. We also include to our analysis measurements of the bulk and envelope metallicities, obtained by fit of interior models on gravitational data from Cassini Grand Finale. These measurements are summarized in Figure 1.

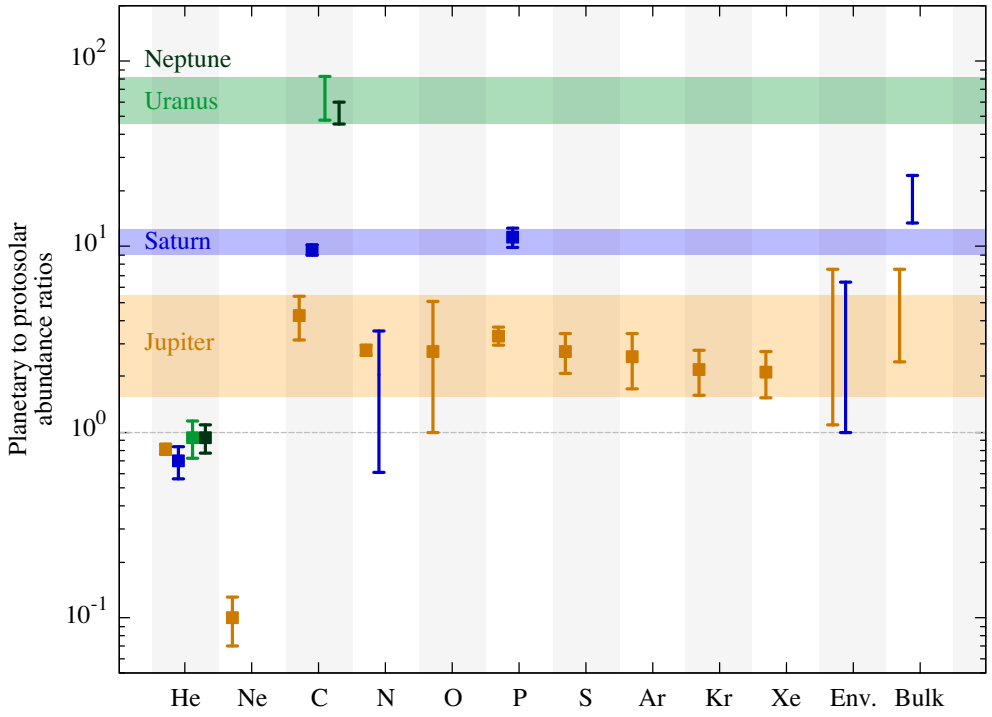

Fig. 1. Composition of giant planets of the Solar System. Adapted from (Aguichine & Mousis 2024, in prep).

2.2 Disk model

The composition of the PSN is computed with the model of Aguichine et al. (2020, 2022). In this model, the disk is mostly made of a H_2-He cloud that is axisymmetric, orbiting the proto-Sun at near-Keplerian frequency Ω_K, and in hydrostatic equilibrium in the vertical direction with a scale height H_g. The surface density Σ_g of H_2-He is evolved according to the formalism of α-viscous disks (Lynden-Bell & Pringle 1974). The disk is filled with 13 trace species: H_2O, CO, CO_2, CH_3OH, CH_4, N_2, NH_3, H_2S, PH_3, Ar, Kr, Xe, and refractory dust. The abundances of trace species are computed from the composition of the protosun (Lodders et al. 2009). Each trace species can exist either in solid or vapor phase. Their surface densities $\Sigma_{sol,i}$ and $\Sigma_{vap,i}$, respectively, evolve following an advection-diffusion equation (Birnstiel et al. 2012; Desch et al. 2017). The two major parameters considered here are the α viscosity, a dimensionless parameter controling the level of turbulence of the H_2-He gas, and the initial CO:CO_2 distribution. We choose values of α ranging from 5×10^{-4} to 5×10^{-3}, based on models calibrated on disk observations (Hartmann et al. 1998; Hueso & Guillot 2005; Desch et al. 2017). Our fiducial case corresponds to CO:CO_2 = 10:30, and we also explore different ice compositions, such as CO:CO_2 = 30:10, as well as the extreme case CO:CO_2 = 40:0 (Boogert et al. 2015; Oberg et al. 2023).

2.3 Model fitting against the data

Our first goal is to investigate where and when the metallicity of Saturn can be reproduced in the disk. When the value of α increases, a higher degree of turbulent mixing results in metallicity peaks that are less prominent and more widely dispersed. When the CO/CO_2 ratio decreases, the enrichment peak of CO at ∼25 AU becomes smaller, and so does the enrichment peak of water at ∼4 AU, since less oxygen is available to form H_2O. The

total metallicity of the PSN (solids+vapors) can match the metallicity of Saturn's envelope (1–5.4 times the solar value) only in the following cases:

- within the water iceline at 0.1–0.5 Myr of the PSN evolution, when α is in 5×10^{-4} – 10^{-3}, and assuming CO:CO_2 = 40:00;
- within the water iceline and at the CO_2 iceline at 0.1–1.0 Myr of PSN evolution, when α is in 5×10^{-4} – 10^{-3} and CO:CO_2 = 30:10 or 10:30;
- within 10 AU when $\alpha = 5 \times 10^{-3}$, which is slightly further than the CO_2 iceline.

The above results justify focusing on the formation of Saturn at the CO_2 iceline. Overall, the most significant enrichment in carbon occurs within the inner region adjacent to the CO_2 iceline, where CO_2 vapors accumulate due to the cold finger effect. To achieve carbon enrichment levels comparable to those found in Saturn's atmosphere (C/H = 9.61 ± 0.59 relative to the solar value), the majority of carbon must exist in the form of CO_2, indicating that it predominantly resides among volatile molecules rather than refractory grains. For the disk properties, values of $\alpha \leq 10^{-3}$ are preferable. A summary of predicted volatile abundances in Saturn's atmosphere are shown in Figure 2.

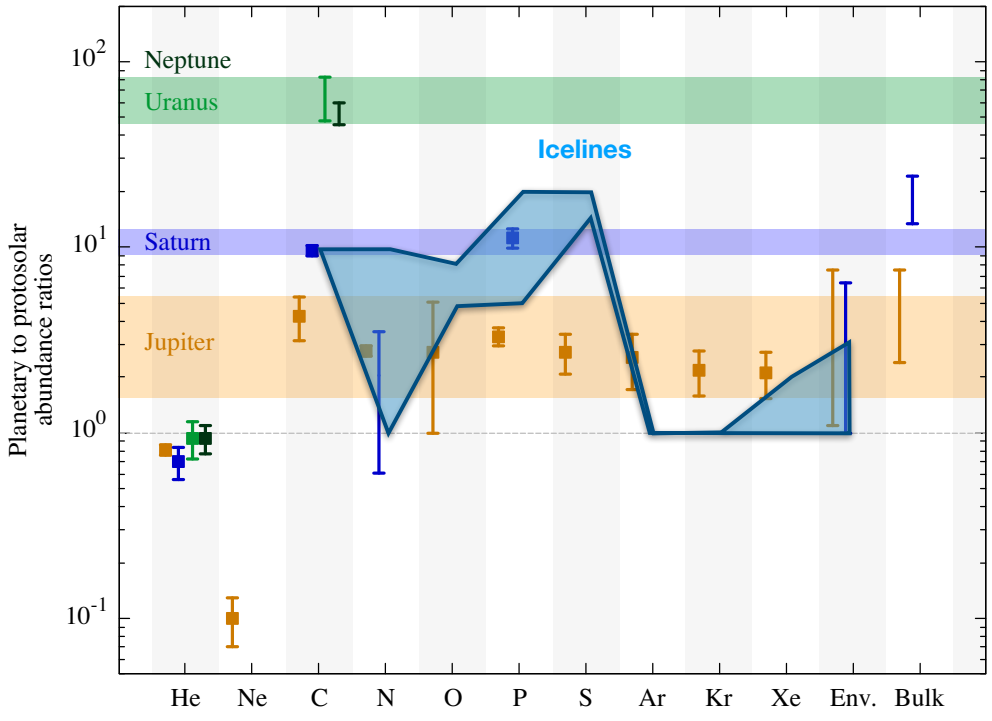

Fig. 2. Summary of the predicted volatile abundances in Saturn's atmosphere according to our model. Adapted from (Aguichine & Mousis 2024, in prep).

3 Conclusions

In this work, we investigated the effect of icelines on the composition of the PSN and how it can reflect on the composition of Saturn. Our goal was to determine at what time and location the composition of the PSN matches the composition of Saturn's atmosphere, while remaining agnostic to formation processes. In particular, our goal was to investigate whether the composition of Saturn's atmosphere and envelope can be explained by formation in the vicinity of the CO_2 or CO iceline.

We find that the metallicity of the PSN can only match the composition of Saturn's envelope, i.e., a heavy element content 1–5.4 times the protosolar value, but not the metallicity of the atmosphere (9–12.5 times

protosolar), nor the bulk metallicity of Saturn (13.5–24.3 times protosolar). We also find that a partitionning favoring CO_2 over CO also better matches the C abundance of Saturn's atmosphere.

The predictions derived from our model are outlined in Figure 2. Noble gases serve as excellent indicators for the formation conditions of giant planets within the solar system (Mandt et al. 2020). We propose that an *in-situ* probe has the potential to definitively discern between different sources of volatiles in Saturn, thereby eliminating the possibility of multiple formation processes simultaneously (Mousis et al. 2022).

This material is based upon work supported by NASA'S Interdisciplinary Consortia for Astrobiology Research (NNH19ZDA001N-ICAR) under award number 19-ICAR19_2-0041.

References

Aguichine, A., Mousis, O., Devouard, B., & Ronnet, T. 2020, ApJ, 901, 97
Aguichine, A., Mousis, O., & Lunine, J. I. 2022, PSJ, 3, 141
Birnstiel, T., Klahr, H., & Ercolano, B. 2012, A&A, 539, A148
Boogert, A. C. A., Gerakines, P. A., & Whittet, D. C. B. 2015, ARA&A, 53, 541
Desch, S. J., Estrada, P. R., Kalyaan, A., & Cuzzi, J. N. 2017, ApJ, 840, 86
Fletcher, L. N., Baines, K. H., Momary, T. W., et al. 2011, Icarus, 214, 510
Fletcher, L. N., Orton, G. S., Teanby, N. A., & Irwin, P. G. J. 2009a, Icarus, 202, 543
Fletcher, L. N., Orton, G. S., Teanby, N. A., Irwin, P. G. J., & Bjoraker, G. L. 2009b, Icarus, 199, 351
Guillot, T. 2005, Annual Review of Earth and Planetary Sciences, 33, 493
Hartmann, L., Calvet, N., Gullbring, E., & D'Alessio, P. 1998, ApJ, 495, 385
Helled, R., Anderson, J. D., Podolak, M., & Schubert, G. 2011, ApJ, 726, 15
Hubickyj, O., Bodenheimer, P., & Lissauer, J. J. 2005, Icarus, 179, 415
Hueso, R. & Guillot, T. 2005, A&A, 442, 703
Levison, H. F., Thommes, E., & Duncan, M. J. 2010, AJ, 139, 1297
Lodders, K., Palme, H., & Gail, H. P. 2009, Landolt Börnstein, 4B, 712
Lynden-Bell, D. & Pringle, J. E. 1974, MNRAS, 168, 603
Mandt, K. E., Mousis, O., Lunine, J., et al. 2020, Space Sci. Rev., 216, 99
Mankovich, C. R. & Fuller, J. 2021, Nature Astronomy, 5, 1103
Militzer, B., Wahl, S., & Hubbard, W. B. 2019, ApJ, 879, 78
Mousis, O., Atkinson, D. H., Ambrosi, R., et al. 2022, Experimental Astronomy, 54, 975
Movshovitz, N., Fortney, J. J., Mankovich, C., Thorngren, D., & Helled, R. 2020, ApJ, 891, 109
Nettelmann, N., Helled, R., Fortney, J. J., & Redmer, R. 2013, Planet. Space Sci., 77, 143
Ni, D. 2020, A&A, 639, A10
Oberg, N., Cazaux, S., Kamp, I., et al. 2023, A&A, 672, A142
Schneider, A. D. & Bitsch, B. 2021, A&A, 654, A72
Vazan, A., Helled, R., Podolak, M., & Kovetz, A. 2016, ApJ, 829, 118